Static and Dynamic Micromagnetics in Finite-Length-Cylindrical Nanowire Y-Junctions

Sergiy M. Bokoch and Stéphane Labbé
Laboratoire Jean Kuntzmann, UMR 5224 CNRS, Tour IRMA, 51 rue des Mathematiques, B.P. 53, 38041 Grenoble Cedex 9, France

Keywords: static and dynamic micromagnetics, nanowires, Y-junctions, ...

PACS: 75.60.Ch, 75.75.+a, ...

Abstract A method is presented to compute...

1 Introduction

For more than century, beginning from Maxwell's pioneering works till nowadays, the electrostatics and electromagnetism of continuous media have been transformed into one of the basic branch of a contemporary physics, namely classical electrodynamics [1, 2]. In spite of a significant progresses of quantum electrodynamics its classical version still plays an important role in fundamental physics and at the applied research frontier. Therefore, in many practical cases the precision of the agreement of the results of classical electrodynamics with experiment is truly astounding [2]. It is worth noting that one of the central part of our current understanding of classical electrodynamics belongs to many outstanding findings in micromagnetics [3-6]. Since founding of fundamentals of static and dynamic micromagnetics (see [3-6] and references therein), and due to the enhanced interest in spintronics this direction has recently initiated the many practical perspective applications in novel multifunctional microelectronics as solid-state magnetic random access memories (MRAMs) [7, 8] and magnetic domain-wall logic devices [9]. One can note that MRAM is a nonvolatile, high density/speed memory technology which is engage in competition with such advanced ones as based on the numerous physical phenomena as phase-change, ferroelectric tunneling, thermochemical, redox-based, magnetoresistive, *etc* [10, 11, 12]. The main idea of MRAM is to build of a mesoscopic architecture of electromagnetic elements [9] incorporated in a certain way into a silicon wafer which operates by the conventional Boolean logic functions such as AND, NOT, and OR/XOR, but with magnetically-induced principle, namely based on the magnetic domain-walls (DWs) or their physical superposition [7, 8]. Thus, the key conception of MRAM or DW-logic microelectronic processing supposes to use 1D or 2D ferromagnetic elements connected between each others into 3D specific functional diagrams. Then, this clever device might work at the certain, usually pulsing (non-uniform), field-induced electromagnetic interaction between the elements. Since the basic conceptions of MRAM [7, 8] and DWs-logic [9] technologies have been proposed the many researchers tried to realize them in practice in view of various possible microelectronic schemes [13, 14, 15, 16, 17, 18, 19]. For example, in Refs. [13, 14, 15, 16, 17] the authors of these works have successfully fabricated a room-temperature NOT gate and magnetic-shift register. This clever device works as follows: the NOT gate consists of ferromagnetic wires, shaped into upside-down Y junction; then, as the DW moves under an external magnetic field up into the stem of the Y junction and down again, it leads to spatial inverting the head to head configuration to the tail to tail configuration or vice versa. Thus, by changing DW configurations, the NOT gate device exchanges a logical '0' for '1' and '1' for '0'. Then, recently, Brien *et al.* [18] have experimentally prepared a bidirectional shift register as an eight-bit data storage based on an open-ended chain of ferromagnetic NOT gates (Y junctions). This device can support bidirectional data flow and comparing to conventional transistor-based logic is reversible and can operate of several modes. Similarly to Ref. [18], Zeng and co-workers [19] have experimentally fabricated asymmetric version of a shift register, optimized on a square grid. As a result, they built a 2D storage scheme by tessellating an elementary data unit.

Naturally and first of all, for uninterrupted operation of such 3D-magnetic logics, one can request to find the reasonable solutions of some fundamental problems from micromagnetics or electrodynamics point of views in general. Thus, completely developed MRAMs and DW-logic might operate by the mesoscopic magnetic DW structure (for instance, Néel or Bloch types), namely its static and dynamic behaviors under influence of the applied electromagnetic fields. In order to meet of these technological conditions we must to understand in detail the following points: (i) equilibrium-static DW structure, (ii) time-dependent evolution parameters of the DW structure, and (iii) all possible types (including their interrelation) of the electromagnetic interactions between the elements used. These requirements (i-iii) should be satisfied for both 'irreducible' structural units as a function of microscopic and mesoscopic parameters, for instance, crystal lattice symmetry, geometry of the particles, *etc* (ferromagnetic nano-bodies as finite-length wires with different cross-sectional view, spheres, cones, ellipsoids, toruses, *etc*) and for their functional/logic junctions (for instance, Y, S, L, C, T, ring- *etc* types). Moreover, in the case of junctions it is very important to define explicitly the 'irreducible' configurations and formulate the transformation 'rules' in order to build of more complex logic structures. It is well known that in the case of bulk magnets there are numerous experimental techniques for investigation of static and dynamic DWs structure, for example, based on the magneto-optical Kerr effect (MOKE), transmission electron microscopy (TEM), magnetic force microscopy (MFM), X-rays od neutrons diffraction methods, *etc* (for details see a famous monograph of Hubert and Schäfer [20]). However, very often for the practical applications, when 1D nanomagnets suppose to be used, especially in the case of MRAM technology, the resolution capability of these direct/indirect experimental methods is not enough to make an unambiguous conclusion on microscopic DWs parameters of the separated low-dimensional magnetic units. In this particular case the classical micromagnetics theory, formulated by Landau and Lifshitz (LL model)

[21] in term of 1D problem and then extended by Brown [3, 4] (see also some salient monographs [5, 6]) for 3D case can successfully be used. Surprisingly, however due to the miniaturization tendency of the electronic engineering components, one arrives to the eccentric conclusion that 1D model becomes even more powerful tool than its 3D prototype under computation and/or prediction their physical functionality.

The static micromagnetic problem for potential DWs-logic nanomagnets has recently been considered independently by various research groups within the scope of both the physical [22-29] and rigorous mathematical methodologies [30-34]. For example, using of Brown's type micromagnetic equations [3, 4], McMichael and Donahue [22] have considered a head to head DW structure in magnetic strips with widths, w, from 75 to 500 nm and thicknesses, t, from 1 to 64 nm. The proper minimization of exchange and magnetostatic energies leads to stabilization of one of two equilibrium DW structures, namely transverse and vortex walls. As a result, the proposed phase diagram demonstrates the lower energy for transverse DWs when dimensions are less than $t_{crit}w_{crit} \approx 130A/\mu_0 M_s^2$ (where A and M_s are the exchange stiffness constant and saturation magnetization of the ferromagnetic materials used). Similarly to [22], Trunk *et al.* [23] have also investigated the DW static transition from Bloch to Néel type in Permalloy films between 160 and 10 nm thickness using direct integration of the Landau-Lifshitz-Gilbert (LLG) equation. It was found that at the thickness of 80 nm, the DW is a symmetric Bloch wall with two adjoining vortices. The Bloch to Néel transition takes place between 35 and 30 nm, below which the DW becomes a symmetric Néel wall. It is worth noting on series of conspicuous works [24-27] where the authors have introduced and theoretically developed a conception of elementary topological magnetic defects with different 'winding' numbers (namely, vortices of ± 1 and/or edge defects of $\pm \frac{1}{2}$ types) for quantitative explanation of complex magnetic patterns observed in ferromagnetic nanostructures of a planar geometry like strips and rings. In other work, Vila *et al.* [28] have presented magnetotransport measurements (angular dependence of the anisotropic magnetoresistance) and micromagnetic simulations for Co cylindrical nanowires of 60 nm in diameter with transverse-magnetocrystalline anisotropy. They found that due to the reducing of demagnetizing energy the magnetic configuration involves two magnetic vortices along the wire with alternate chirality. The nucleation, core-reversal and annihilation of this vortex state are analyzed at different stage of hysteresis cycle. Finally, the authors emphasize the importance of the anisotropic properties and geometry for reversal processes in such nanomagnets. In addition, Zeng *et al.* [29] have recently investigated the magnetostatic charge distribution of Néel type DW in prismatic permalloy nanowires with a width between 40 and 200 nm and thickness of 5 nm. They have shown that the charge distribution is very asymmetric in 200 nm wide wire, however becomes less so as a width is reduced to 40 nm, where the exchange energy term plays an important role (see also [22, 23]). On the other hand, the several important and mathematically rigorous generalizations of the conventional LL 1D static problem [21] have been recently proposed [30-34]. In spite of some mathematical loss of simplicity, these models are mostly analytic and consequently their results do not suffer from many computational problems which take place at solving the LL or LLG equations, and, therefore, in some particular cases they may probably predict better the general micromagnetic behaviors of the objects of interest.

Since we know a solution of a static problem [22-34] for certain ferromagnetic nanobodies ('irreducible' structural units), the detailed understanding of the DW dynamics in these nanomagnets will be the next important step (for simplicity we discuss an influence of the external magnetic field only). For the first time in 1956, Walker [35] has developed a 1D analytical model for magnetic DW dynamics thus *ipso facto* founds the DW dynamics in micromagnetics (see also an exhaustive analysis in [6]). The equations of motion of a 180 ^{o} DW (Bloch type wall) in an infinite medium with uniaxial anisotropy under an external dc magnetic field have elegantly been derived. The analytical solution of the equation of motion demonstrates that above the critical field, H_W (Walker breakdown field), the DW *linear* velocity behaves according to the time-oscillatory mode and below H_W has a linear dependence. Some recent generalizations and improvements of the Walker DW dynamics model as well as novel experimental observations can be found elsewhere [36, 37, 38, 39, 40, 41, 42, 43]. For example, using the numerical calculations, Thiaville *et al.* [36] have studied the static DW structure and its dynamic behaviors under an external magnetic field applied along the 1D and 2D nanowires with axial magnetization. It is shown that the static DW structure and its dynamics in nanowires with diameters as large as several exchange lengths are very similar to 1D Bloch DW and are very sensitive to the value of a damping parameter, α and transverse anisotropy. The results proposed by Walker [35] for 1D Bloch DW dynamics are completely confirmed. Furthermore, the non-trivial simulation results have been obtained by Nakatani *et al.* [37]. Using numerical micromagnetic simulations the authors have shown that for rough strip edges, the DW velocity breakdown, H_W, is suppressed. For instance, at roughness larger than the exchange length (9 nm for a 5 nm thickness of a wire) is optimal to get a maximal DW velocity. Despite the large wire width compared with the exchange length, roughness stabilizes fast DW motion up to larger fields. Finally, it was concluded that roughness should rather be engineered than avoided when fabricating nanostructures for DW propagation. Then, on the basis of spatially resolved dynamic MOKE measurements, Beach *et al.* [38] have investigated in detail the dynamics of field-driven DW propagation in ferromagnetic nanowires over a broad field range up to 70 Oe. They tested the nanowires with thickness of 600 nm and with length of 20 μm. The authors have found a linear $v-H$ dependence up to a Walker breakdown, followed by a region of negative differential mobility, $\partial v/\partial H < 0$, and irregular DW motion. At higher fields ($H > H_i$, where H_i denotes the DW injection field), v is again linear with H, but with lower average mobility. Yang *et al.* [39] have investigated both experimentally (based on the high-speed MOKE measurements) and theoretically (analytically in the case of a 1D model and numerically solving the LLG equation in the case of nanowire with a thickness of 20 nm) the magnetic DW velocity oscillations in permalloy nanowires. It is worth noting that above breakdown ($H > H_W$), the DW velocity varies periodically with time and thus leading to an oscillatory trajectory of a DW along a wire as was predicted before by Walker [35]. In order to observe such oscillations the authors have experimentally investigated the transient broadening of the Kerr signal produced by a DW sweeping across the MOKE beam-spot. Wang *et al.* [40] have generalized an existent DW dynamics model [35] and developed a new theory of magnetic field-induced DW propagation in a finite magnetic nanowire with a rectangular cross-section A. As a result a proper definition of DW propagation velocity was proposed, and a velocity-field formula for high-field (above H_W) has been analytically derived. It is shown, like in [36], that the theory is valid for an arbitrary DW structure (Bloch or Néel type) and allows to estimate the DW velocity in a reasonable way even when the DW is not homogenously moving. Results based on the presented analytical formula beyond the Walker breakdown field are in excellent agreement with both experiments and numerical simulations. Yan *et al.* [41], on the basis of LLG equation, have demonstrated that circularly polarized magnetic fields (CPMF) at gigahertz frequency can efficiently drive a DW to propagate along a magnetic nanowire. As a result, two motion modes are found, namely (i) rigid DW propagation at low frequency ($\omega < \omega_C$, where ω_C is the critical frequency; it is similar to the Walker breakdown field, H_W) and (ii) oscillatory propagation at high frequency ($\omega > \omega_C$). It is also found that DW motion under a CPMF is equivalent to the DW motion under a uniform spin current in the current perpendicular to the plane magnetic configurations, at the same time the CPMF frequency plays the role of the current. The further important extension of DW dynamics model in nanowires has been proposed by Min *et al.* [42]. Using an extended LLG representation they have taken into account the effect of magnetic disorder (for example, caused by the spatial micro-heterogeneities as roughness, thickness, *etc*) into domain vortex dynamics, namely by means of introducing of saturation magnetization fluctuations, D. As a result, the authors have pointed out that in the present of magnetic fluctuations, the DW velocity increases as such a disorder increases for $H > H_W$, while for $H < H_W$ the DW velocity decreases ($\upsilon_{DW} \sim 1/\alpha$) due to the increasing of effective damping parameter, α. One should also be mentioned on significant results in DW dynamics recently reported in work of Lewis *et al.* [43]. The authors of this paper have shown experimentally (on the basis of MOKE measurements) that a series of cross-shaped traps (a comb structure with two center-to-center spacing $d = 150$ and 200 nm) acts to prevent transformations of the DW structure (to inhibit the nucleation of antivortices) under an external magnetic field and thus increase the DW velocity by a factor of four compared to the maximum velocity on a plain strip. They achieve DW speeds of up to 1550 m s^{-1} for $d = 150$ nm and 940 m s^{-1} for $d = 200$ nm in the fields about 40 Oe and 73 Oe, respectively.

With regard to static and dynamic micromagnetic problems in various nanowire junctions it is worth noting series of works [44, 45, 46, 47, 48, 49, 50, 51]. For example, domain nucleation processes in 'uniaxial' wire junctions [44], DWs pinning in L-type nanowire junctions created by constrictions and protrusions [45] and in T-type nanowire junctions [46], operational functionality of S-type rectangular thin-film elements [47], magnetostatic interaction between two oppositely charged transverse DW in adjacent U-shaped nanowires [48], experimental analysis of DWs pinning in curved nanostrips [49], and DWs pinning/depinning in a three terminal ferromagnetic Y-junctions [50, 51] have been in detail investigated.

2 Micromagnetics Model of Cylindrical Nanowire Y-junctions

2.1 Demagnetization Field: *A Semi-phenomenological Analysis*

It is well known that one of the main difficulty during developing of the self-consistent micromagnetism theory, even in the case of uniformly magnetized bodies is a demagnetization tensor field (DTF). The calculation of this field or demagnetizing tensor N_{ij} is of fundamental importance for quantitative analysis of the magnetometric energy of a magnetized bodies. There are well known analytic solution of this problem exceptionally for the certain simple geometry, namely for a sphere, infinite and finite cylinder and for ellipsoid (see [5] and refs. therein). At the same time it is worth to noting on very recent works deal with a computation of the DTF for an arbitrary particle shape [52, 53, 54, 55, 56]. In Ref. [52] Bellegia *et al.* proposed a Fourier space approach (similarly to Kachaturyan's formulation in the case of consideration of long-range elastic interactions in mixed solids [57]) to compute the DTF. As a result, the authors have explicitly demonstrated that this approach allows to calculate analytically the DTF for a broad class of nanoparticles, in particular, all the faceted (polyhedral) particles as well as 'rotational' ones and some bodies with a high degree of a symmetry. This capable scheme has been elegantly formulated in terms of so-called 'shape' function or 'shape' amplitude, $D(\mathbf{k})$, of nanoparticles [52]. Later on, in Ref. [53], Tandon *et al.* have presented the analytic form of explicit shape amplitudes $D(\mathbf{k})$ for sphere, some particles with general polyhedral shape, rectangular prism, regular tetrahedron and hexagonal plate, truncated paraboloid, cone truncated by spherical cap, and they have also considered in details the case of DTF as well as expressions for magnetostatic energy for arbitrary objects with a cylindrical symmetry. In contrast to Ref. [53] in Ref. [54], Tandon *et al.* have compared the results of numerical approach with analytical one proposed before in Ref. [53]. They have concluded that both methods are in good agreement. The further exhaustive extension of the Fourier space approach has been developed in details by Beleggia *et al.* for the cases of general ellipsoid [55] and uniformly polarized torus [56].

Due to the fact that demagnetization field is proportional to the volume of the magnetized body, let us consider the several important volumes, formed the Y-junctions, namely: sphere, Ω_s, and segments' volumes, Ω_{segm}, forming by 3D cross-section of a sphere and cylindrical nanowires (Fig. 1). Here, the two possible configurations are presented in Fig. 1. The case I presents the unchangeable configuration of Y-junction with $\theta = 2\pi/3$. For this configuration

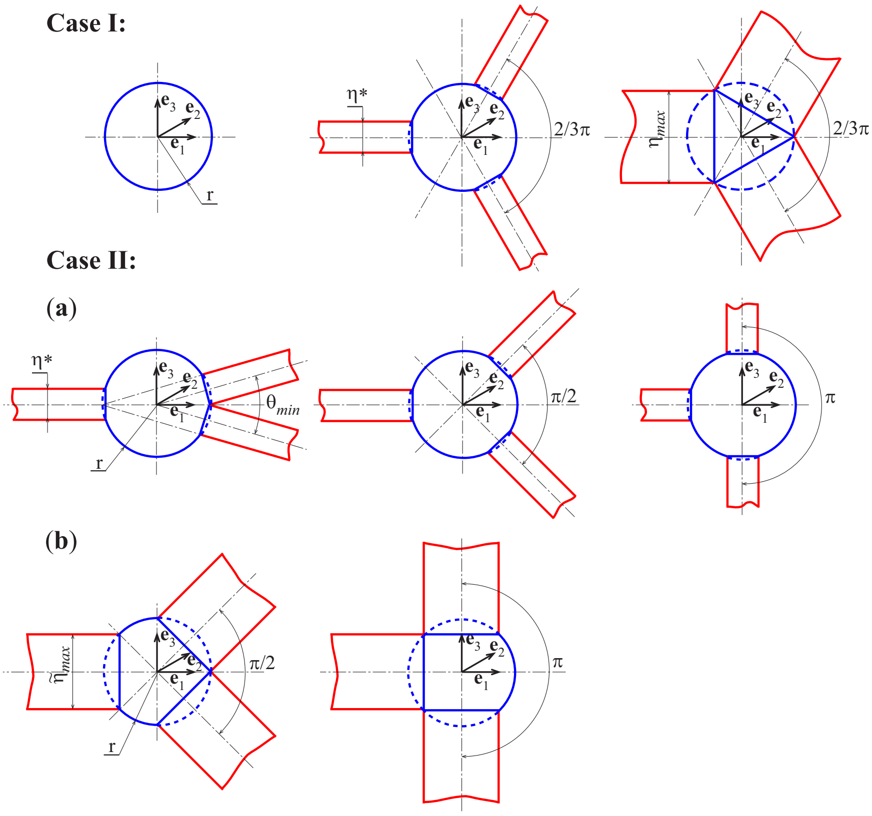

Figure 1:
Generalized Y-type junction of finite-length-cylindrical nanowires. Case I: $\eta = [0, \eta_{max}], \theta = 2\pi/3 = \text{const}$, Case II: (a) $\theta = [\theta_{min}(\eta), \pi], \eta = \eta^* = \text{const}$, and (b) $\theta = [\pi/2, \pi], \eta = \widetilde{\eta}_{max} = \text{const}$. $\mathbf{e}_1, \mathbf{e}_2, \mathbf{e}_3$ are the unit vectors within the Cartesian coordinate system.

the maximal diameter of nanowires, η_{max}, will be defined as $\eta_{max} = r\sqrt{3}$, thus, η changes within the interval $[0, r\sqrt{3}]$ (where r is the radius of a sphere). The case II (a,b) shows its flexible configuration, in general, with $\theta = [\theta_{min}, \pi]$, where η changes within the another interval $[0, r\sqrt{2}]$. Consequently, when $\theta \to \pi$ Y-junction transforms into T-junction. Thus, the important parameters for our calculations are the ratio of Ω_{segm}/Ω_s and the critical angle θ_{min} as a function of η and r.

The volume of a sphere is

$$\Omega_s = \frac{4}{3}\pi r^3. \tag{1}$$

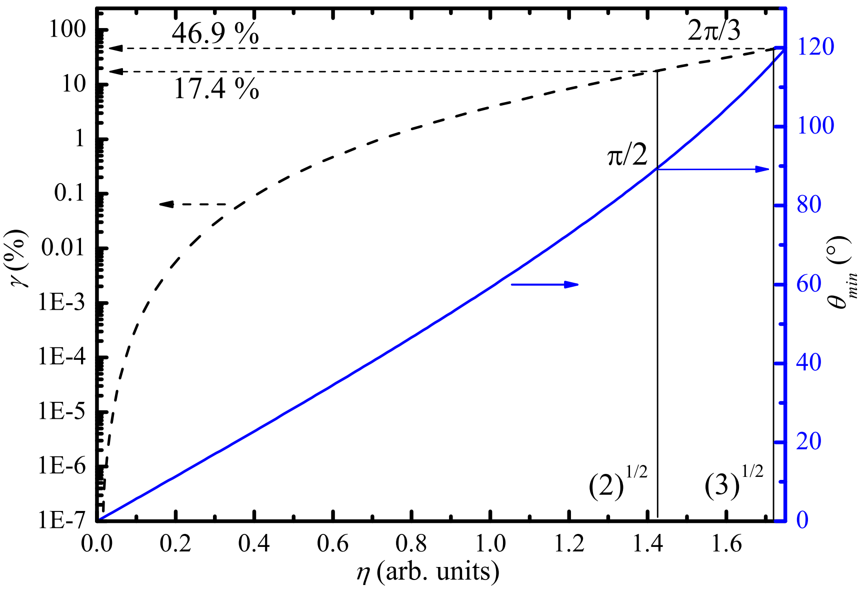

Figure 2:
Dependencies of coefficient γ and θ_{min} as a function of η for generalized Y-junctions shown in Fig. 1. Here we assume $r = 1$. For clarity the axis of γ is presented in the logarithmic scale.

The volume of a cross-sectional segment is

$$\Omega_{segm} = \frac{1}{3}\pi h^2(3r - h), \tag{2}$$

where h is the height of a segment which can be defined as

$$h = r - \sqrt{r^2 - \eta^2/4}. \tag{3}$$

Substituting Eq. (3) into Eq. (2) we immediately get

$$\Omega_{segm} = \frac{\pi}{3}\left(2r^3 - 2r^2\sqrt{r^2 - \eta^2/4} - \frac{\eta^2}{4}\sqrt{r^2 - \eta^2/4}\right). \tag{4}$$

Let introduce the coefficient γ, which defines the ration between volumes of segments and sphere, in the following form

$$\gamma = \frac{N\Omega_{segm}}{\Omega_s} \cdot 100\%, \tag{5}$$

where N is the number of nanowires; in the case of Y-junctions $N = 3$. Finally, we get the general expression for coefficient γ for three-terminal Y-junction in the following form

$$\gamma = \frac{3}{2}\left(1 - \frac{1}{r}\sqrt{r^2 - \eta^2/4} - \frac{1}{8}\frac{\eta^2}{r^3}\sqrt{r^2 - \eta^2/4}\right) \cdot 100\%. \tag{6}$$

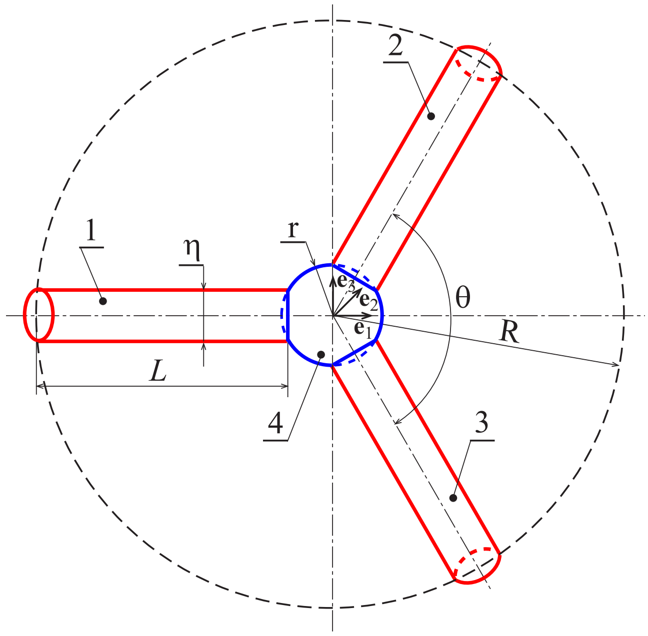

Figure 3:
Generalized Y-type junction of finite-length-cylindrical nanowires. $i = 1, 2, 3$ is the number of nanowires, 4 is the truncated sphere of a radius of r, $R = \sigma_{\eta,r} + L$.

It is worth noting, that in order to avoid a crossing between nanowires (for instance, as considered in the case II(a) in Fig. 1.) we have to define the minimally possible angle between them as a function of Y-junction geometry. This relation can be written as

$$\theta_{min} = 2 \arctan \left(\frac{\eta}{2\sqrt{r^2 - \eta^2/4}} \right). \tag{7}$$

Graphical representation of functions $\gamma(\eta)$ and $\theta_{min}(\eta)$, calculated according to Eqs. (6,7), is presented in Fig. 2. As it can be seen in Fig. 2, the angle θ_{min} depends significantly on η, whereas, the coefficient γ changes slowly. For example, for the ration of $\eta/r = 1, \frac{1}{2}, \frac{1}{5}$ the coefficient γ and θ_{min} are 3.9, 0.2, 0.01% and 60, 29, 11.5°, respectively. Thus, one can conclude that at the ratio of $\eta/r = \frac{1}{5}$ the magnetostatic influence of cross-sectional segments can be neglected with respect to the sphere and wires contributions. At the same time, the value of $\theta_{min} = 11.5°$ is in a good agreement with experimental results of Refs. [50, 51]. Therefore, for further calculations we accept this ratio.

2.2 Static Micromagnetic Model

According to the conventional micromagnetics model [1, 3, 4, 5] the general expression for magnetic energy of a ferromagnetic body with an arbitrary shape is

$$E(u) = \frac{A}{2}\int_{\Omega} |\nabla u|^2 dx + \frac{1}{2}\int_{\mathbb{R}^3} |h_d(u)|^2 dx - \int_{\Omega} h_{ext} \cdot u dx, \tag{8}$$

where A is the exchange stiffness constant, h_d and h_{ext} are the demagnetizing and external magnetic fields, respectively.
Similarly to Eq. (1), the volume of a sphere can then be re-written as

$$\Omega_s = B_3(0, r).$$

From Fig. 3 it is clear that for each ith nanowires the following condition is valid

$$\omega_L =]\sigma_{\eta,r}, L[\times B_2(0,\eta), \quad \text{where} \quad \sigma_{\eta,r} = \sqrt{r^2 - \eta^2/4},$$

so then

$$\widetilde{\omega}_L = B_3(0,r) \cap \omega_{i,L}.$$

In the general case

$$\forall i \in \{1, ..., n\}, \ \theta_i \in [0, 2\pi],$$

when, for instance,

$$\theta_1 < \theta_2 < ... < \theta_n,$$

and rotation of a separated ith nanowire, R_{θ_i}, around the e_1 axis can be presented in the form

$$R_{\theta_i} x = \begin{pmatrix} 1 & 0 & 0 \\ 0 & \cos\theta_i & -\sin\theta_i \\ 0 & \sin\theta_i & \cos\theta_i \end{pmatrix} x. \tag{9}$$

So then we can write

$$\omega_{i,L} = R_{\theta_i}\omega_L, \widetilde{\omega}_{i,L} = R_{\theta_i}\widetilde{\omega}_L.$$

In this case the total cross-sectional volume of a sphere with nth nanowires is

$$\Omega_{\eta,r} = \Omega_s \cup \left(\bigcup_{i=1}^{n} \omega_{i,L} \right). \tag{10}$$

In Eq. (8) we assume that $\forall u \in H^1(\Omega_{\eta,r}, \mathbb{R}^3), \quad h_{ext} \in L^\infty(\Omega_{\eta,r}, \mathbb{R}^3)$, then we can write

$$\begin{cases} rot(h_d(u)) = 0, \\ div(h_d(u)) = -div(\widetilde{u}) \text{ in the sense of } \mathfrak{D}'(\mathbb{R}^3; \mathbb{R}^3), \end{cases} \tag{11}$$

where $\widetilde{u}$ defines as

$$\widetilde{u} = \begin{cases} u & \text{in} \quad \Omega_{\eta,r}, \\ 0 & \text{in} \quad \mathbb{R}^3 \backslash \Omega_{\eta,r}. \end{cases} \tag{12}$$

The demagnetizing filed can be expressed as

$$\forall x \in \mathbb{R}^3, \quad h_d(u(x)) = -\frac{1}{4\pi} \nabla div \int_{\mathbb{R}^3} \frac{\widetilde{u}(x)}{|x-y|} dy. \tag{13}$$

Let us consider the two asymptotic behaviors:
H_1 ($L = \infty$; see Fig. 3): In this case it is easy to conclude

$$\begin{cases} \forall i \in \{1, ..., n\}, \quad \forall (x_2, x_3) \in B_2(0, \eta), \\ \lim\limits_{x_1 \to \infty} u \left(R_{\theta_i} \begin{pmatrix} x_1 \\ x_2 \\ x_3 \end{pmatrix} \right) = 0. \end{cases} \tag{14}$$

The second aimed state, H_2, should be realized when $\eta \to 0$ (see Fig. 3). So then we can write

$$\begin{cases} u(R_{\theta_i}(x)) = u(R_{\theta_i}(x) e_1), \quad \text{when} \quad e_1 = R_{\theta_i} e_1 \\ \forall x \in \Omega_s, \quad u(x) \text{ is valued in } S^2. \end{cases} \tag{15}$$

Thus let us write all the main energy contributions entering into Eq. (8) for Y-junction shown in Fig. 3.
It is evident that the exchange energy contribution for ith nanowire can be written as

$$\forall i \in \{1, ..., n\} \quad E_{ex} = \frac{A}{2} \int_{\omega_{i,L}} |\nabla u|^2 dx = \frac{A}{2} \int_{\sigma_{\eta,r}}^{\infty} \left| \frac{\partial u}{\partial x} (R_{\theta_i}(x)) \right|^2 dx, \tag{16}$$

The all possible demagnetizing contributions induced by 'field-elements' magnetic interactions are as follow

$$\forall i \in \{1, ..., n\} \quad E^1_{demag} = \frac{1}{2} \int_{\omega_{i,L}} |u \cdot e_i|^2 dx, \tag{17}$$

$$\forall i \in \{1, ..., n\} \quad E^2_{demag} = -\frac{1}{2} \int_{\omega_{i,L}} u \cdot \left(\sum_{j \neq i}^{n} h_d(u|_{\omega_{j,L}}) \right) dx, \tag{18}$$

$$E^3_{demag} = -\frac{1}{2} \int_{\Omega_{\eta,r}} u \cdot h_d(u|_{\Omega_{\eta,r}}) dx, \tag{19}$$

$$\forall i \in \{1, ..., n\} \quad E^4_{demag} = -\frac{1}{2} \int_{\omega_{i,L}} u \cdot h_d(u|_{\Omega_{\eta,r}}) dx. \tag{20}$$

$$E^5_{demag} = -\frac{1}{2}\int_{\Omega_{\eta,r}} u\cdot h_d\left(u|_{\bigcup_{i=1}^n \omega_{i,L}}\right)dx. \tag{21}$$

The external field contribution has a conventional form, namely

$$E_{ext} = -\int_\Omega u\cdot h_{ext} dx. \tag{22}$$

Thus, finally, take into account Eqs. (16,17,18,19,20,21,22) we arrive to the expression for the total magnetic energy of a generalized nth-terminal junction of nanowires in the following form

$$E_{\eta,r}(u) = \frac{A}{2}\sum_{i=1}^{n}\int_{\sigma_{\eta,r}}^{\infty}\left|\frac{\partial u}{\partial x}(R_{\theta_i}(x))\right|^2 dx + \frac{1}{2}\int_{\omega_{i,L}}|u\cdot e_i|^2 dx$$

$$-\frac{1}{2}\int_{\omega_{i,L}} u\cdot\left(\sum_{j\neq i}^{n} h_d(u|_{\omega_{j,L}})\right)dx - \frac{1}{2}\int_{\Omega_{\eta,r}} u\cdot h_d(u|_{\Omega_{\eta,r}})dx$$

$$-\frac{1}{2}\int_{\omega_{i,L}} u\cdot h_d(u|_{\Omega_{\eta,r}})dx - \frac{1}{2}\int_{\Omega_{\eta,r}} u\cdot h_d\left(u|_{\bigcup_{i=1}^n \omega_{i,L}}\right)dx - \int_\Omega u\cdot h_{ext}dx. \tag{23}$$

It is worth noting that in the case of a conventional three-terminal Y-junctions Eq. (23) becomes simpler ($n = 3$).

2.3 Numerical Calculations Results

2.4 Domain Walls Dynamics in Y-junctions

DWs width can be expressed as

$$\Delta = \sqrt{A/(K_u + \pi M_s^2)},$$

where A is the exchange stiffness constant, K_u is the uniaxial anisotropy constant, M_s is the saturation magnetization.

$$m_x = \tanh(x/\Delta), m_y = 1/\cosh(x/\Delta).$$

Let us consider the conventional Landau-Lifshitz equation to model the precessional motion of magnetization $\mathbf{m}$ in a magnetic solid under an effective magnetic field $\mathbf{H}_{eff}$ and with damping. This ordinary differential equation is

$$\frac{\partial \mathbf{m}}{\partial t} = -\gamma\mathbf{m}\times\mathbf{H}_{eff} - \frac{\alpha}{M_s}\mathbf{m}\times(\mathbf{m}\times\mathbf{H}_{eff}),$$

where α is the Landau-Lifshitz phenomenological damping parameter, γ is the classical electron gyromagnetic ration and $\mathbf{H}_{eff} = \mathbf{H}(\mathbf{m}) + \mathbf{H}_a$ ($\mathbf{H}_a$ is the applied magnetic field in general case of an arbitrary form). The possible types

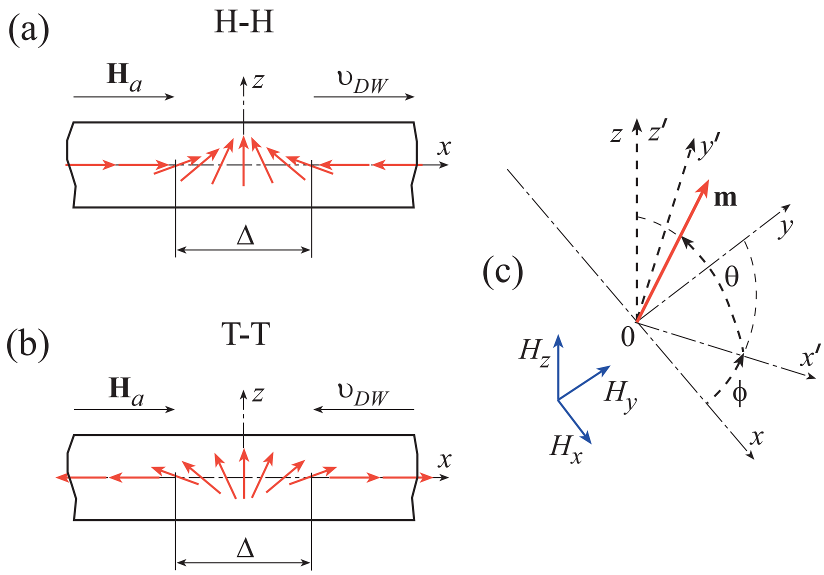

Figure 4:
Dynamics of head-to-head (H-H) (a) and tail-to-tail (T-T) (b) DWs in magnetic nanowires. (c) Cartesian (x, y, z) and two orthogonal polar $(0z, \phi), ((0y', \theta))$ coordinate systems' representations of DMs dynamics. Here $\mathbf{H}_a$ is the external applied magnetic field of a general form (H_x, H_y, H_z), Δ and υ_{DW} are the DWs width and velocity, respectively.

of DWs and generalized magnetic moment in magnetic bodies are presented in Fig. 4. As can be seen from Fig. 4(c), it is more convenient to consider the DWs dynamics problem in a polar coordinate system. Let us as usual assume that $\mid \mathbf{m} \mid= 1$ (where $\mathbf{m} = m_x\mathbf{e}_1 + m_y\mathbf{e}_2 + m_z\mathbf{e}_3$). Consequently, we can write the following relations between Cartesian components of $\mathbf{m}$ and polar angles θ, ϕ

$$\begin{cases} m_x = \sin\theta\cos\phi, \\ m_y = \sin\theta\sin\phi, \\ m_z = \cos\theta. \end{cases} \tag{24}$$

3 Conclusions

In a given work we...

Acknowledgement
One of the authors (S.M.B) is grateful to the Nanoscience Foundation (France) for partial financial support of the present work. Also we would like to thank Prof. M. Beleggia (Center for Electron Nanoscopy at DTU, Denmark) for kindly providing his own publications on analytic magnetostatics in magnetized nano-bodies.

References

[1] L. D. Landau, and E. M. Lifshitz, *Electrodynamics of continuous media. In Course of theoretical physics*, vol. 8, Pergamon Press, Oxford, 1960.

[2] J. D. Jackson, *Classical Electrodynamics*, 3rd Ed., Wiley, New York, 1999.

[3] W. F. Brown Jr., *Magnetostatic principles in ferromagnetism*, The Netherlands, North-Holland, 1962.

[4] W. F. Brown Jr., *Micromagnetics*, Interscience Publishers, John Wiley & Sons, New York-London, 1963.

[5] A. Aharoni, *Introduction to the Theory of Ferromagnetism*, 2nd Ed., Oxford Univ. Press Inc., New York, 2000.

[6] H. Suhl, *Relaxation Processes in Micromagnetics*, Oxford Univ. Press Inc., New York, 2007.

[7] S. S. P. Parkin, U.S. Patents 6.834.005, 6.898.132, 6.920.062, 7.031.178, and 7.236.386 (2004 to 2007).

[8] S. S. P. Parkin, M. Hayashi, and L. Thomas, Magnetic Domain-Wall Recetrack Memory, Science **320**, 190-194 (2008).

[9] D. A. Allwood, G. Xiong, C. C. Faulkner, D. Atkinson, D. Petit, and R. P. Cowburn, Magnetic Domain-Wall Logic, Science **309**, 1688-1692 (2005).

[10] G. I. Meijer, Who Wins the Nonvolatile Memory Race?, Science **319**, 1625-1626 (2008).

[11] R. Waser, R. Dittmann, G. Staikov, and K. Szot, Redox-Based Resistive Switching Memories - Nanoionic Mechanisms, Prospects, and Challenges, Adv. Mater. **21**, 2632-2663 (2009).

[12] P. Zubko, and J.-M. Triscone, A leak of information, Nature **460**, 45-46 (2009).

[13] D. A. Allwood, G. Xiong, M. D. Cooke, C. C. Faulkner, D. Atkinson, N. Vernier, and R. P. Cowburn, Submicrometer Ferromagnetic NOT Gate and Shift Register, Science **296**, 2003-2006 (2002); see also viewpoint in: Science **296**, 1948 (2002).

[14] D. A. Allwood, G. Xiong, M. D. Cooke, C. C. Faulkner, D. Atkinson, and R. P. Cowburn, Characterization of submicrometer ferromagnetic NOT gates, J. Appl. Phys. **95**, 8264-8270 (2004).

[15] X. Zhu, D. A. Allwood, G. Xiong, R. P. Cowburn, and P. Grutter, Spatially resolved observation of domain-wall propagation in a submicron ferromagnetic NOT-gate, Appl. Phys. Lett. **87**, 062503-1-3 (2005).

[16] D. A. Allwood, G. Xiong, and R. P. Cowburn, Magnetic domain wall serial-in parallel-out shift register, Appl. Phys. Lett. **89**, 102504-1-3 (2006).

[17] D. A. Allwood, G. Xiong, and R. P. Cowburn, Domain wall cloning in magnetic nanowires, J. Appl. Phys. **101**, 024308-1-4 (2007).

[18] L. O'Brien, D. E. Read, H. T. Zeng, E. R. Lewis, D. Petit, and R. P. Cowburn, Bidirectional magnetic nanowire shift register, Appl. Phys. Lett. **95**, 232502-1-3 (2009).

[19] H. T. Zeng, D. Read, L. O'Brien, J. Sampaio, E. R. Lewis, D. Petit, and R. P. Cowburn, Asymmetric magnetic NOT gate and shift registers for high density data storage, Appl. Phys. Lett. **96**, 262510-1-3 (2010).

[20] A. Hubert, and R. Schäfer, *Magnetic Domains: The Analysis of Magnetic Microstructures*, Springer, New York, 1998.

[21] L. D. Landau, and E. M. Lifshitz, On the theory of the dispersion of magnetic permeability in ferromagnetic bodies, Phys. Z. Sowjetunion **8**, 153-169 (1935).

[22] R. D. McMichael, and M. J. Donahue, Head to head domain wall structures in thin magnetic strips, IEEE Trans. Magn. **33**, 4167-4169 (1997).

[23] T. Trunk, M. Redjdal, A. Kákay, M. F. Ruane, and F. B. Humphrey, Domain wall structure in Permalloy films with decreasing thickness at the Bloch to Néel transition, J. Appl. Phys. **89**, 7606-7608 (2001).

[24] O. Tchernyshyov, and G.-W. Chern, Fractional Vortices and Composite Domain Walls in Flat Nanomagnets, Phys. Rev. Lett. **95**, 197204-1-4 (2005).

[25] F. Q. Zhu, G. W. Chern, O. Tchernyshyov, X. C. Zhu, J. G. Zhu, and C. L. Chien, Magnetic Bistability and Reversal of Asymmetric Ferromagnetic Nanorings, Phys. Rev. Lett. **96**, 027205-1-4 (2006).

[26] H. Youk, G.-W. Chern, K. Merit, B. Oppenheimer, and O. Tchernyshyov, Composite domain walls in flat nanomagnets: The magnetostatic limit, J. Appl. Phys. **99**, 08B101-1-3 (2006).

[27] G.-W. Chern, H. Youk, and O. Tchernyshyov, Topological defects in flat nanomagnets: The magnetostatic limit, J. Appl. Phys. **99**, 08Q505-1-3 (2006).

[28] L. Vila, M. Darques, A. Encinas, U. Ebels, J.-M. George, G. Faini, A. Thiaville, and L. Piraux, Magnetic vortices in nanowires with transverse easy axis, Phys. Rev. B **79**, 172410-1-4 (2009).

[29] H. T. Zeng, D. Petit, L. O'Brien, D. Read, E. R. Lewis, and R. P. Cowburn, The influence of wire width on the charge distribution of transverse domain walls and their srtay field interactions, J. Magn. Magn. Mater. **322**, 2010-2014 (2010).

[30] G. Carbou, and S. Labbé, Stability for static walls in ferromagnetic nanowires, Discrete and Continuous Dynamical Systems, Series B **6** 273-290 (2006).

[31] G. Carbou, and S. Labbé, and E. Trélat, Control of travelling walls in a ferromagnetic nanowire, Discrete and Continuous Dynamical Systems, Series S **1**, 51-59 (2008).

[32] G. Carbou, and S. Labbé, and E. Trélat, Smooth control of nanowires by means of a magnetic field, Communications on Pure and Applied Analysis **8**, 871-879 (2009).

[33] G. Carbou, and S. Labbé, Stabilization of walls for nano-wires of finite length, European Series in Applied and Industrial Mathematics: Control, Optimisation and Calculus of Variations, forthcoming 2010.

[34] S. Labbé, Y. Privat, and E. Trélat, Stability properties of steady-states for a network of ferromagnetic nanowires, *submitted* 2011.

[35] L. R. Walker, Bell Telephone Laboratories memorandum (1956): unpublished; N. L. Schryer, and L. R. Walker, The motion of 180^o domain walls in uniform dc magnetic fields, J. Appl. Phys. **45**, 5406-5421 (1974).

[36] A. Thiaville, J. M. Garcia, and J. Miltat, Domain wall dynamics in nanowires, J. Magn. Magn. Mater. **242-245**, 1061-1063 (2002).

[37] Y. Nakatani, A. Thiaville, and J. Miltat, Faster magnetic walls in rough wires, Nature **2**, 521-523 (2003).

[38] G. S. D. Beach, C. Nistor, C. Knutson, M. Tsoi, and J. L. Erskine, Dynamics of field-driven domain-wall propagation in ferromagnetic nanowires, Nature **4**, 741-744 (2005).

[39] J. Yang, C. Nistor, G. S. D. Beach, and J. L. Erskine, Magnetic domain-wall velocity oscillations in permalloy nanowires, Phys. Rev. B **77**, 014413-1-4 (2008).

[40] X. R. Wang, P. Yan, and J. Lu, High-field domain wall propagation velocity in magnetic nanowires, Europhys. Lett. **86**, 67001-p1-p5 (2009).

[41] P. Yan, and X. R. Wang, Domain wall propagation due to the synchronization with circularly polarized microwaves, Phys. Rev. B **80**, 214426-1-4 (2009).

[42] H. Min, R. D. McMichael, M. J. Donahue, J. Miltat, and M. D. Stiles, Effects of Disorder and Internal Dynamics on Wall Propagation, Phys. Rev. Lett. **104**, 217201-1-4 (2010).

[43] E. R. Lewis, D. Petit, L. O'Brien, A. Fernandez-Pacheco, J. Sampaio, A.-V. Jausovec, and H. T. Zeng, Fast domain wall motion in magnetic comb structures, Nature **9**, 980-983 (2010); Also see viewpoint in: G. Beach, Beyond the speed limit, Nature **9**, 959-960 (2010).

[44] W. Y. Lee, C. C. Yao, A. Hirohata, Y. B. Xu, H. T. Leung, S. M. Gardiner, S. McPhail, B. C. Choi, D. G. Hasko, and J. A. C. Bland, Domain nucleation processes in mesoscopic $Ni_{80}Fe_{20}$ wire junctions, J. Appl. Phys. **87**, 3032-3036 (2000).

[45] D. Petit, A.-V. Jausovec, D. Read, and R. P. Cowburn, Domain wall pinning and potential landscapes created by constrictions and protrusions in ferromagnetic nanowires, J. Appl. Phys. **103**, 114307-1-6 (2008).

[46] D. Petit, A.-V. Jausovec, H. T. Zeng, E. Lewis, L. O'Brien, D. Read, and R. P. Cowburn, Mechanism for domain wall pinning and potential landscape modification by artificially patterned traps in ferromagnetic nanowires, Phys. Rev. B **79**, 214405-1-9 (2009).

[47] T. Hesjedal, and T. Phung, Magnetic logic element based on an S-shaped Permalloy structure, Appl. Phys. Lett. **96**, 072501-1-3 (2009).

[48] L. O'Brien, D. Petit, H. T. Zeng, E. R. Lewis, J. Sampaio, A.-V. Jausovec, D. E. Read, and R. P. Cowburn, Near-Field Interaction between Domain Walls in Adjacent Permalloy Nanowires, Phys. Rev. Lett. **103**, 077206-1-4 (2009).

[49] E. R. Lewis, D. Petit, L. Thevenard, A.-V. Jausovec, L. O'Brien, D. E. Read, and R. P. Cowburn, Magnetic domain wall pinning by a curved conduit, Appl. Phys. Lett. **95**, 152505-1-3 (2009).

[50] C. Nam, Y. Jang, K.-S. Lee, and B. K. Cho, Characteristics of domain wall pinning and depinning in a three-terminal magnetic Y-junction, Nanotechnology **19**, 015703-1-4 (2008).

[51] C. Nam, Y. Jang, K.-S. Lee, and B. K. Cho, Current-driven output magnetization switching in a magnetic nanowire with three-terminal Y junction, Appl. Phys. Lett. **92**, 202501-1-3 (2008).

[52] M. Beleggia, and M. De Graef, On the computation of the demagnetization tensor field for an arbitrary particle shape using a Fourier space approach, J. Magn. Magn. Mater. **263**, L1-L9 (2003).

[53] S. Tandon, M. Beleggia, Y. Zhu, and M. De Graef, On the computation of the demagnetization tensor for uniformly magnetized particles of arbitrary shape. Part I: Analytical approach, J. Magn. Magn. Mater. **271**, 9-26 (2004).

[54] S. Tandon, M. Beleggia, Y. Zhu, and M. De Graef, On the computation of the demagnetization tensor for uniformly magnetized particles of arbitrary shape. Part II: numerical approach, J. Magn. Magn. Mater. **271**, 27-38 (2004).

[55] M. Beleggia, M. De Graef, and Y. Millev, Demagnetization factors of the general ellipsoid: An alternative to the Maxwell approach, Phil. Mag. **86**, 2451-2466 (2006).

[56] M. Beleggia, M. De Graef, and Y. T. Millev, Magnetostatics of the uniformly polarized torus, Proc. R. Soc. A **465**, 3581-3604 (2009).

[57] A. G. Khachaturyan, *Theory of Structural Transformations in Solids*, John Wiley & Sons, New York, 1983.